C. R. Chimie 19 (2016) 1527–1534

Contents lists available at ScienceDirect

Comptes Rendus Chimie

www.sciencedirect.com

Full paper/Mémoire

Type 2 diabetes and uric acid stones: A powder neutron diffraction investigation

Diabète de type 2 et calculs d'acide urique: une étude par diffraction de neutrons

Michel Daudon [a, b, *], Emmanuel Letavernier [a, b], Raphael Weil [c], Emmanuel Véron [d], Guy Matzen [d], Gilles André [e], Dominique Bazin [c, f]

[a] *AP-HP, Hôpital Tenon, Service des explorations fonctionnelles, 75020 Paris, France*
[b] *Unité INSERM UMR S 1155, UPMC, Hôpital Tenon, 75020 Paris, France*
[c] *Laboratoire de physique des solides, UMR 8502, Université Paris-Sud, Bât 510, 91405 Orsay cedex, France*
[d] *CNRS-CEMHTI, 1D, avenue de la Recherche-Scientifique, 45071 Orléans cedex 2, France*
[e] *Laboratoire Leon-Brillouin, (CEA–CNRS) Saclay, Gif-sur-Yvette cedex 91191, France*
[f] *CNRS, LCMCP-UPMC, Collège de France, 11, place Marcellin-Berthelot, 75231 Paris cedex 05, France*

ARTICLE INFO

Article history:
Received 20 February 2015
Accepted 21 April 2015
Available online 20 December 2015

Keywords:
Nephrolithiasis
Uric acid
Type 2 diabetes
Neutron diffraction
Gender

ABSTRACT

Recent epidemiologic investigations have identified an association between type 2 diabetes and uric acid kidney stones. This association was more apparent in women than in men. In this paper, we show through powder neutron diffraction that particle sizes of uric acid kidney stones were significantly different between male and female patients (84.7 ± 5.3 vs. 140.2 ± 6.7 nm, $p = 0.000003$). Interestingly, when type 2 diabetes appeared, this structural difference between male and female vanished (76.1 ± 3.9 vs. 78.8 ± 4.2 nm, not significant). Thus, the complete set of structural data is in line with observations regarding epidemiological data. Some explanations based on supersaturation are discussed.

1. Introduction

Significant changes in dietary habits and lifestyle during the past thirty years have induced a considerably increased incidence of obesity, metabolic syndrome and type 2 diabetes throughout the world [1–7]. At the same time, urolithiasis relentlessly increased [8–17] affecting now up to 15% of the population in industrialized countries [3,18,19].

Two recent epidemiological investigations [20,21] point out an intimate correlation between these public health problems, namely obesity, type 2 diabetes and urolithiasis. Unfortunately, the chemical nature of the stones was not recorded. At this point, we should recall that the chemistry of such concretions is quite complex, involving various inorganic and/or organic compounds: Ca oxalate (70% of the cases), Ca and Mg phosphates (15%), uric acid (10%) and other phases (5%) which can be organized into different crystalline phases [22–27]. The chemical composition, colour and morphology constitute key information which helps in the determination of the associated pathology [28–41]. As suggested by recent reports, calcium oxalate and uric acid (UA) stones may be favoured by metabolic disorders associated with metabolic syndrome or type 2 diabetes [42–44]. However, the dramatic increase in the proportion of UA stones observed in stone-formers

* Corresponding author.
E-mail address: michel.daudon@tnn.aphp.fr (M. Daudon).

http://dx.doi.org/10.1016/j.crci.2015.04.006

suffering these pathologies underlines the special link between insulin resistance and UA stone formation in both male and female patients. From a medical point of view, several pathophysiological arguments may explain the propensity of stone-formers with type 2 diabetes to produce UA stones. Metabolic syndrome alters cell sensitivity to insulin and renal acid–base metabolism, resulting in a lower urine pH and an increased risk of uric acid stone disease [3,45]. With respect to gender, some authors have observed that women had a stronger association of diabetes with the risk of prevalent kidney stones than did men, and that the former appear especially at risk of forming UA stones [46]. Taking advantage of the large number of patients referred to our hospital laboratory, a more precise relationship has been established between UA or 2,6,8-trioxypurine ($C_5H_4N_4O_3$) kidney stones and pathology. The complete set of data shows that the proportion of UA stones is strikingly higher in stone formers with diabetes than those without [47,48], which is in agreement with the data reported by other authors [49].

The aim of this paper is to provide a structural description of uric acid stones in order to determine whether diabetic and non-diabetic patients form similar urinary stones. Also, the gender and age of the patients, which seem to be significant parameters, are taken into account in this study. For the sake of clarity, we use the terms 'nanocrystals' and 'crystallites' following Van Meerssche & Feneau-Dupont [50] in order to define the structural hierarchy of these mineral concrements [51–56]. In this simplified scheme, a collection of nanocrystals (each measuring about one hundred nanometres) constitutes a crystallite (measuring some tens of micrometres). Structural characteristics regarding the nanocrystals are provided by powder neutron diffraction (PND) [57–60]. The fact that the neutron interacts only weakly with the stones and thus can penetrate deeply into the bulk [61] offers an excellent opportunity for measuring the average size of the nanometre scale nanocrystals made of light elements as shown for other species identified in kidney stones [62–66]. Regarding crystallites, a precise description of their shape and their structural organization has been performed through Scanning Electron Microscopy (SEM) [67].

2. Materials and methods

2.1. Samples

Regarding UA urinary stones, the classification performed through their morphology as well as by Fourier-Transform InfraRed (FT-IR) spectroscopy [68,69] distinguishes two morphological types, namely IIIa and IIIb, each being related to specific conditions [28]. For example, the surface of IIIa type stones is homogeneous, smooth or slightly embossed. Such IIIa stones are mainly associated with stasis with a moderately low urinary pH and are commonly observed in the bladder of elderly men with prostate hypertrophy. At the mesoscopic scale, these stones are characterized by a very compact inner structure made of concentric layers with a radial organization of the crystals. In contrast, IIIb stones are essentially related to hyperuricosuria and/or very acidic urine as observed in the metabolic syndrome and type 2 diabetes. Their surface is heterogeneous, rough or porous and their colour varies from whitish to brownish-red. Their cross-section exhibits a loose, porous, and poorly organized structure.

The stones selected for the present study fulfilled the following criteria: (1) the sample size of the stone was large enough to perform all the analytical methods including stereomicroscopy examination, FT-IR analysis and thereafter SEM and PND measurements; (2) clinical data regarding the patient's age and diabetes status, (3) the anatomical location of the stone at the time of removal (upper urinary tract: kidney, ureter; or lower urinary tract: bladder).

UA stones from 43 patients (24 males, 19 females) were investigated (Tables 1–3). All the stones were mainly composed of uric acid anhydrous (UAA). The mean age of the patients was 58.8 ± 2.8 for females and 66.9 ± 2.5 years for males ($p = 0.036$). Among these patients, 22 (11 males, 11 females) suffered from type 2 diabetes (Table 3). A preliminary analysis was carried out at the hospital using a stereomicroscope for morphological typing and an FT-IR spectrometer to determine accurate stone composition.

All statistical comparisons including UAA crystal size versus the patient's sex and age, the anatomical location of the stone at the time of removal and the stone morphology were performed using ANOVA or a chi square test when appropriate. Data analysis was performed with the NCSS statistical package (J. Hintz, Gainesville, FL). A p value less than 0.05 was considered as statistically significant.

2.2. Investigation tools

An FEI/Philips XL40 environmental SEM (ESEM) equipped with an energy-dispersive X-ray spectrometer was used for sample characterization. An important feature of the ESEM compared to a conventional SEM is the fact that non-conductive materials can be imaged without any conductive coating, which permits a direct observation

Table 1
Estimated particle size (±standard deviation) in nm of UAA crystals determined through PND for non-diabetic male patients.

Sample	Localisation – Age (years)	Estimated size of UAA crystals (±standard deviation) in nm	
		Non diabetic males Type IIIa stones	Non diabetic males Type IIIb stones
1-14222	L	65 (2)	
2-26297	L – 79	83 (7)	
3-33096	L – 69	76 (7)	
4-39613	L – 91	97 (3)	
5-9291	L – 78	88 (2)	
6-35866	U – 61		81 (4)
7-39514	U – 34		109 (3)
8-40161	U – 66		69 (2)
9-43605	U – 60		73 (3)
10-46063	U – 44		73 (3)
11-56883	U – 51		112 (5)
12-55521	U – 44		81 (3)
13-46015	L – 67		93 (3)

L: lower urinary tract; U: upper urinary tract.

Table 2
Estimated particle size (±standard deviation) in nm of anhydrous uric acid crystals determined through PND for non-diabetic female patients

Sample	Localisation – Age (years)	Estimated size of UAA crystals (±standard deviation) in nm	
		Non diabetic females Type IIIa stones	Non diabetic females Type IIIb stones
14-26093	U – 48	144 (13)	
15-33951	U – 70	107 (8)	
16-37223	U – 64	185 (14)	
17-42754	U – 62	143 (10)	
18-24808	U – 34		146 (8)
19-25765	U – 72		130 (5)
20-30297	U – 49		110 (5)
21-38727	U – 56		155 (10)

U: upper urinary tract.

with no damage to the sample. Imaging was performed with a gaseous secondary electron detector, at an accelerating voltage of 20 kV and a water pressure of 0.4 torr in the chamber. This low pressure was used to maintain a high spatial resolution for the X-ray analysis by minimizing the scattering of the primary electron beam. Also, a Zeiss SUPRA55-VP type scanning electron microscope was used for microstructure observation. This field effect gun microscope operates at 0.5–30 kV. High resolution observations were obtained using two secondary electron detectors: an in-lens and an Everhart–Thornley detector.

Neutron diffraction diagrams were collected on a G4.1 two-axis multidetector powder diffractometer [70] installed at the cold-source beamline of the Orphée reactor (Saclay, France). This beamline was equipped with a two-axis powder diffractometer with a vertically focussing pyrolytic graphite monochromator and an 800-cell multidetector covering an 80° 2θ range (step 0.1° between 2 cells). Neutron diffraction patterns were collected at room temperature between 7 and 87° using a wavelength of 2.4226 Å, with an acquisition time of the order of a few hours, the exact value depending on the samples. This particular experimental setup offers the opportunity of determining the size of nanocrystals in a range between 5 and 200 nm.

Table 3
Estimated particle size (±standard deviation) in nm of UAA crystals determined through PND for diabetic patients

Sample	Localisation – Age (years)	Estimated size of UAA crystals (±standard deviation) in nm	
		Diabetic Males	Diabetic Females
22-4021	U – 60	65 (4)	
23-5432	U – 79	84 (3)	
24-19381	L – 79	87 (3)	
25-26273	L – 76	83 (3)	
26-43019	U – 50	98 (5)	
27-44050	U – 59	62 (4)	
28-44336	U – 79		74 (2)
29-46893	U – 73		80 (3)
30-56617	L – 73		78 (5)
31-57420	L – 60		59 (5)
32-59315	L – 76		66 (6)
33-15216	U – 62		76 (2)
34-30951	U – 61		76 (4)
35-17619	U – 76		87 (3)
36-24951	U – 66		68 (5)
37-26115	U – 56		90 (4)
38-47159	U – 60		63 (4)
39-66145	U – 61		111 (3)
40-57052	U – 41		71 (3)
41-58253	U – 61		82 (3)
42-59028	U – 60		63 (2)
43-38011	U – 58		80 (2)

L: lower urinary tract, U: upper urinary tract.

The phase identification, lattice constant determination and quantitative phase analysis were performed through Rietveld refinement using the Fullprof program [71] based on the crystallographic structure of two reference compounds, namely uric acid dihydrate (UAD), $C_5H_2N_4O_3 \cdot 2H_2O$ [72] which is orthorhombic with a space group Pnab ($a = 0.7409(1)$ nm, $b = 1.7549(3)$ nm, $c = 0.6332(1)$ nm) and UAA ($C_5H_2N_4O_3$), a monoclinic structure with a space group P21/a with four molecules in a unit cell of dimensions $a = 1.4464$ nm, $b = 0.7403$ nm, $c = 0.6208$ nm, $\beta = 65.10°$ [73].

The particle size is determined by extracting the broadening of Bragg peaks of the kidney stone atomic structure due to their finite size [74]. The lower the size, the more the peaks are broadened in comparison to their normal width linked to the resolution function of the neutron diffractometer. We have taken a model of isotropic broadening with a Thomson-Cox-Hastings profile peak function. With the Fullprof program, we refine a Y Lorentzian broadening parameter simply linked to the mean particle size of the compound (**29**). Taking into account the experimental resolution of the beamline G4.1 as well as the signal to noise ratio, the size of the UAA crystals is given by 8.9/Y nm. In this work, only the particle size of the major component, namely UAA, is discussed.

3. Results

Uric acid stones may present mainly two different morphological aspects at the macroscopic scale as illustrated in Fig. 1.

The structural characteristics at the mesoscopic scale obtained by ESEM are presented in Fig. 2. Fig. 2(a) displays the microstructures of a stone belonging to the IIIa morphological type and Fig. 2(b) shows a stone exhibiting a IIIb type.

In Fig. 2(a), a preferential orientation of the crystallites is clearly observed at the 50 μm scale. In a stone corresponding to the IIIb type of our classification, no preferential orientation of the crystals is seen: as an example, a collection of crystallites with random orientation is visualized for the sample as shown in Fig. 2(b) at approximately the same scale. These results are in line with the morphological classification used in routine practice, in which this type of stone exhibits an unorganized macroscopic structure. The distribution of the stones according to their anatomical location showed that type IIIa calculi were more frequent in the bladder (57.9%) while type IIIb calculi were more frequent in the upper urinary tract (95.8% of cases, $p < 0.0001$). However, from the complete set of ESEM images, it was not possible to define any structural differences

Fig. 1. Uric acid calculi. A) surface of a type IIIa stone. The surface is smooth and homogeneous; B) section of a type IIIa stone exhibiting a well organized structure; C) surface of a type IIIb stone. The surface is heterogeneous, locally embossed, rough or porous; D) section of a type IIIb stone exhibiting a poorly organized structure with porous areas. Bars = 3 mm.

between samples from either male or female, diabetic or non-diabetic patients.

The structural investigation at the nanometre scale was performed through PND. PND is a non-destructive tool which has the ability to penetrate deeply inside most materials. The estimated nanocrystal size is thus an average over all nanocrystals present in the kidney stone. We also take advantage of the high sensitivity of the neutrons to light elements, namely hydrogen, oxygen and carbon. Fig. 3 presents a typical PND spectrum of uric acid anhydrous.

Uric acid stones may be formed either in the upper urinary tract or in the bladder, particularly in older male patients with a benign prostate hypertrophy responsible for urine stasis [75]. Comparison of the size of UAA crystals according to the stone location within the urinary tract showed a tendency toward smaller crystals in the lower urinary tract: 78.7 ± 8.0 nm vs. 96.2 ± 5.0 nm for stones developed in the kidney ($p = 0.07$). Another unexpected variation in the size of UAA crystals was observed as a function of the patient's age. The mean crystal size decreased from 106.2 ± 7.3 nm in subjects aged below 60 years to 87.0 ± 6.4 nm ($p = 0.06$) in subjects aged above 70 years.

We report in Figs. 4 and 5 the average size of the nanocrystals measured for non-diabetic male and female patients (Fig. 4: samples 1 to 13 for male patients; Fig. 5: samples 14 to 21 for female patients). Numerical values are reported in Tables 1 (males) and 2 (females).

For males, the average size was 79.2 ± 3.9 nm for IIIa calculi and 82.6 ± 4.3 nm for IIIb calculi ($p = 0.56$), while for females, the average size was 121.8 ± 14.4 nm for IIIa and 96.7 ± 9.8 nm for IIIb calculi ($p = 0.18$). Thus, no difference was found in the crystal size between IIIa and IIIb types. In contrast, the average size for the whole series of UA stones from male patients was 80.7 ± 5.3 nm while for females it was 104.7 ± 6.0 nm ($p = 0.0049$), a strong difference which suggests that the biochemical environment is very different according to the gender of the patient.

Interestingly, in diabetic patients (Table 3, Fig. 6), the mean size of UAA crystals was significantly lower than in non-diabetic patients (77.5 ± 5.3 nm vs. 105.8 ± 5.4 nm, $p = 0.0006$). Indeed, the difference was essentially the result of a change in the crystal size between non-diabetic and diabetic females (140.2 ± 6.8 nm vs. 78.8 ± 5.8 nm, respectively, $p = 0.000003$), while the crystal size remained essentially unchanged in male patients (84.7 ± 3.7 nm in non-diabetic vs. 76.0 ± 4.1 nm in diabetic subjects, $p = 0.2$).

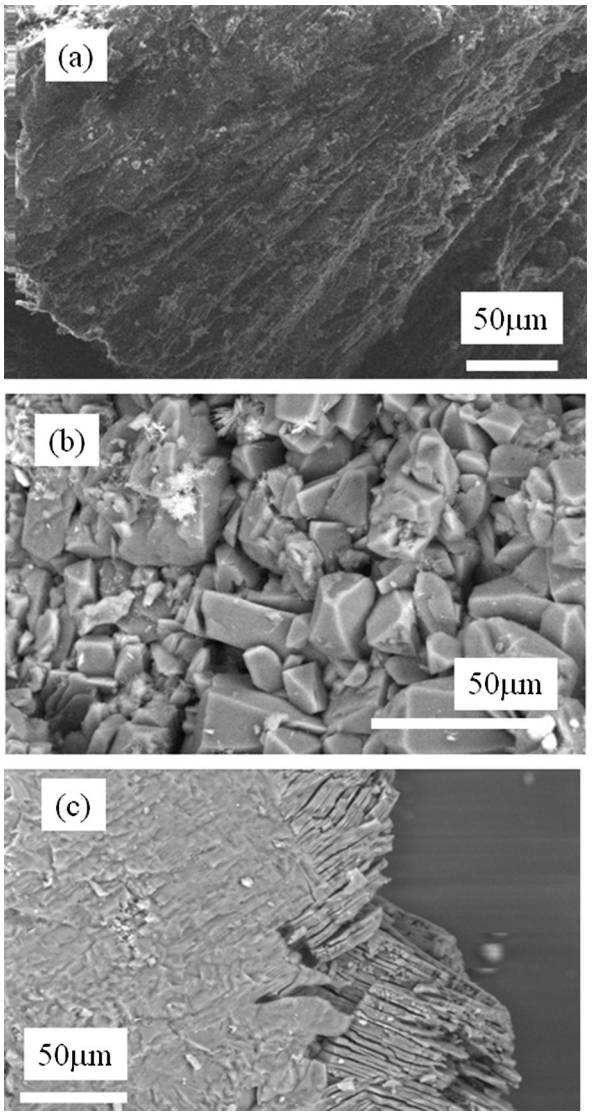

Fig. 2. (a) ESEM image of a IIIa sample showing a preferential orientation of the crystallites, (b) a random orientation of crystallites observed for a IIIb stone (sample N10416) and (c) a specific structure corresponding to the phase conversion between the two uric acid species (from dihydrate to anhydrous).

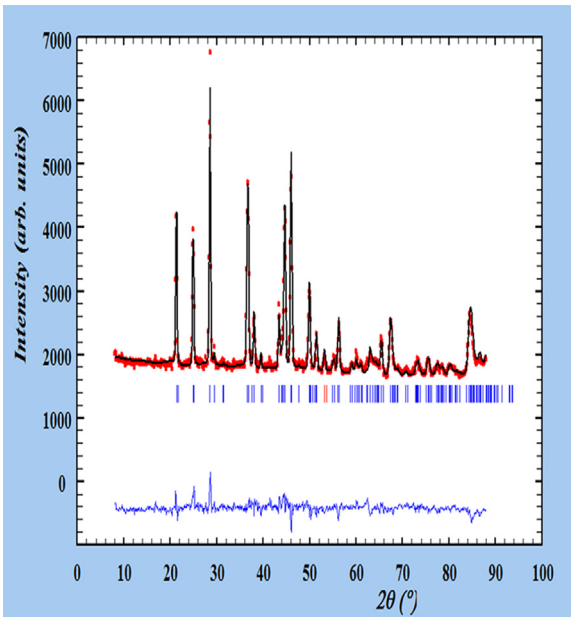

Fig. 3. Final refinement, with experimental (°), calculated (–) and different PND patterns of the sample N 40161. Tick marks below the profiles indicate the peak positions of allowed Bragg reflections for UAA.

4. Discussion

In this study, two different analytical approaches were applied to stone analysis, first ESEM for studying the inner structure and crystallite organization within the stones, and second, PND for measuring the mean size of UAA crystals.

ESEM has been used as an investigation tool in numerous in vitro as well as in vivo investigations [76]. The former helps to describe the morphology of crystals as a function of supersaturation [77], phase conversion processes [78,79], or the effect of uric acid seeds on calcium oxalate formation [80]. Regarding in vivo studies, this technique can reveal the presence of bacteria at the surface of uroliths [81]. Recently, a close relationship was observed between the presence of bacterial imprints, indicative of a past or current urinary tract infection, and both the presence of amorphous carbonated calcium phosphate (or whitlockite) and a high carbonate concentration in calculi made of carbapatite [82]. Such microscopic investigations can play a key role in the diagnosis of major genetic pathologies, revealing a particular crystalline structure in whewellite stones resulting from primary hyperoxaluria type 1 when compared to the common type of whewellite stones [33]. Finally, we use this technique to understand the genesis of Randall's plaque, a deposit of apatite at the surface of the papilla which serves as a nidus for calcium oxalate calculi and also to determine the calcium oxalate calculi growth process at the surface of Randall's plaque [83]. In the present study, we found correlations between the organization of crystallites of uric acid at the mesoscopic scale and macroscopic characteristics of the stones as previously reported for other types of stones. We found a statistical difference between IIIa and IIIb stones according to their anatomical location, IIIa stones being more frequent in the bladder while IIIb stones were essentially formed in the upper urinary tract. However, we failed to find differences between ESEM images and clinical data.

From a clinical point of view, uric acid stones account for 10–20% of urinary calculi in western countries (10% in France) and may be related either to low urine pH or increased excretion of uric acid. Recent epidemiological studies have clearly shown a relationship between overweight, type 2 diabetes and the risk of developing nephrolithiasis [20,21,84]. Other studies underlined an increased risk of uric acid nephrolithiasis as a consequence of metabolic changes in overweight and diabetic patients [49,85,86]. In our experience, pathological changes related

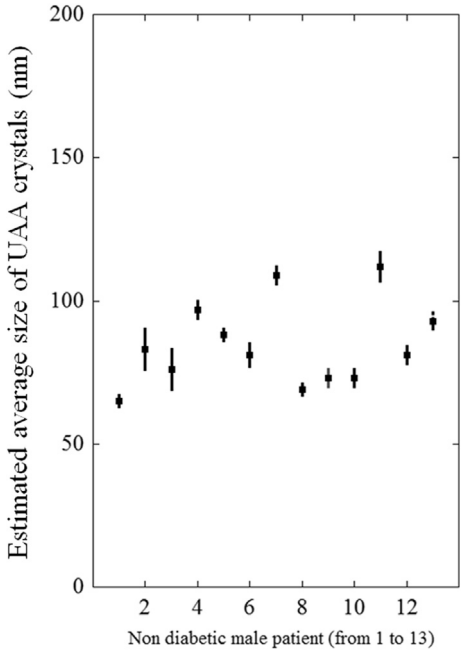

Fig. 4. Nanocrystal sizes of UAA urinary stones from non-diabetic male patients (see Table 1).

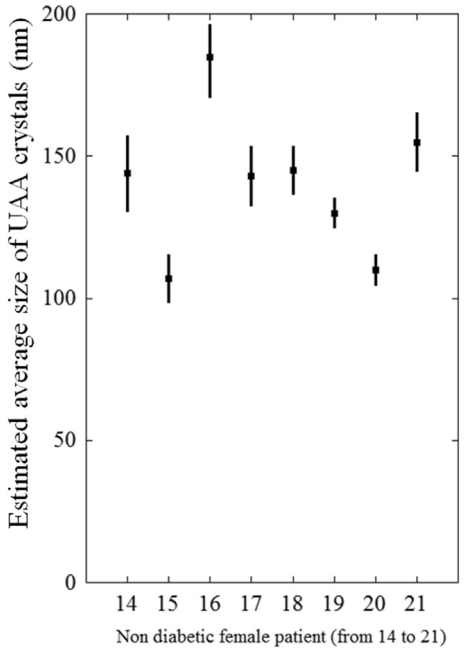

Fig. 5. Nanocrystal sizes of UAA urinary stones from non-diabetic female patients (see Table 2).

to insulin resistance are a major concern in uric acid urolithiasis since about 2/3 of all uric acid stones are associated with the metabolic syndrome or type 2 diabetes [87]. Although the stone composition was considered in some studies [44,48,85] the structural characteristics of the stones were never assessed. The aim of our study was to

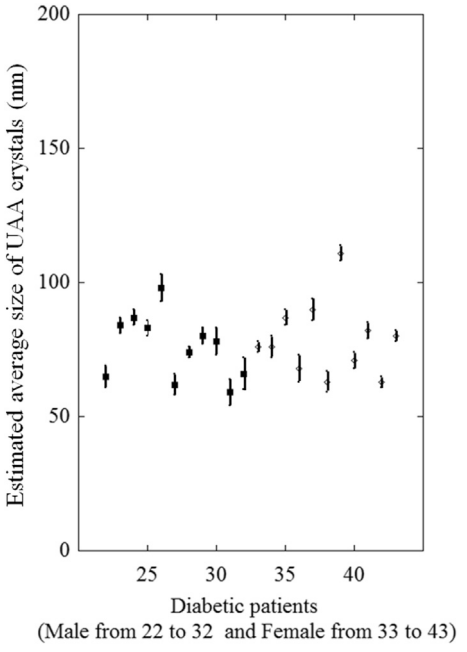

Fig. 6. Nanocrystal sizes of UAA urinary stones from diabetic male (from 22 to 32 in black square) and female (from 33 to 43, white diamonds) patients.

seek possible structural differences at the nanometre and mesoscopic scale in uric acid stones developed in non-diabetic and diabetic male and female patients. At the mesoscopic scale, we were able to differentiate two main types of UA stones according to their crystallite organization. These results are in close agreement with previous descriptions by other authors [79]. These authors also defined two kinds of uric acid stones: type I includes stones with a small central core and a compact columnar uric acid anhydrous shell while type II is associated with porous stones without inner structure. Types I and II of this classification correspond to types IIIa and IIIb stones, respectively in our own classification. We found such a structural organization in both male and female patients. Type IIIb stones appeared clearly more frequent in the upper urinary tract while IIIa stones were more frequent among bladder calculi. Of note, in our series, all bladder stones were from male patients. No structural difference was found between UA stones from male and female patients or between stones from diabetic and non-diabetic patients.

In contrast, one of the striking points of the PND results was that the crystal size of uric acid stones was significantly lower in diabetic patients (77.5 ± 5.3 nm vs. 105.8 ± 5.4 nm, $p = 0.0006$). As previously reported, overweight and obese conditions, one of the main anthropometric characteristics of patients suffering a metabolic syndrome with an insulin resistance, are often associated with an increased risk of UA stones [21,34,85,86]. The main explanation is that insulin resistance could be responsible for a low urine ammonium excretion and a high net acid excretion inducing a decreased urine pH [86]. An inverse correlation between body weight and urine pH has been recently reported [45] and also between HbA1c level in blood and urine pH in patients with

type 2 diabetes [88]. Insulin resistance may also result from a mitochondrial dysfunction, which progressively appears with increasing age, explaining, together with increased body mass index (BMI) related to age, the higher proportion of uric acid observed in elderly patients [89,90].

A low urine pH is the main factor explaining high UA supersaturation in urine and, in clinical practice, acidic urine was the main disorder explaining UA stone formation [91]. These features can explain the high proportion of UA stones in older patients [92]. In accordance with crystallization rules [93], a high UA supersaturation could be responsible for a high number of UA nuclei leading to a smaller size of the observed crystals. Surprisingly, we found a striking difference in the crystal size between male and female patients. Thus, the difference in crystal size observed between diabetic and non-diabetic patients appeared to be essentially related to the patient's sex. A hypothesis is that such a difference between male and female patients could be related to basic differences in urine supersaturation regarding uric acid. From an epidemiological point of view, males are well known to be more prone to developing UA stones than females, the risk increasing with age [94–97].

As shown in Fig. 7, although male and female patients exhibit an increasing proportion of UA stones related to their BMI, only male patients appear to be especially susceptible to that risk.

A possible explanation could be a difference in urine pH between males and females. In our experience, based on urinary pH measurement in more than 20,000 urine samples, females exhibit a significantly higher urine pH than males (6.27 ± 0.02 vs. 6.14 ± 0.01, $p < 0.0001$). This experimental fact suggests that in patients suffering a metabolic syndrome, females are less prone than males to produce very acidic urine, explaining their lower propensity to form uric acid stones.

In the case of type 2 diabetes, the structural difference in crystal size between males and females vanishes. Indeed, among male stone formers, the increased risk of developing UA stones in the case of type 2 diabetes appeared limited when compared to overweight non-diabetic patients; as previously shown, the proportion of uric acid stones in obese male patients (BMI $\geq$ 30 kg/m^2) was 28.7% [48] and moderately increased to 33.2% in diabetic patients [46]. In contrast, in female stone formers, the proportion of uric acid stones increased from 6.1% in the case of normal BMI to 17.1% in obese patients, always remaining significantly lower than in males. Thus, as shown in Fig. 7, female patients seem to be less susceptible to that risk than are male patients, which is in agreement with previous data [48]. The striking point of our previous studies was that the risk of producing uric acid stones among diabetic female stone formers was very high (42.5%) [44]. Such observations suggest that UA supersaturation could be higher in diabetic female patients, while it could be lower in non-diabetic ones, resulting in a smaller number of UAA crystals with a larger size than that observed in male patients. A lower supersaturation also decreases the crystallization rate, inducing a lower risk of crystal retention in the urinary tract [93]. This hypothesis could explain the lower prevalence of UA stones in non-diabetic women, including obese patients. In contrast, in the case of type 2 diabetes, female stone-formers are especially at risk of UA stones, due to high urine UA supersaturation, as suggested by epidemiological data [44] and by PND measurements showing a significant decrease in UA crystal size. Perhaps, in addition to low urine pH, these patients have a higher excretion rate of uric acid in urine than do male subjects and they reach an especially high degree of uric acid supersaturation. Further studies are required to confirm this hypothesis.

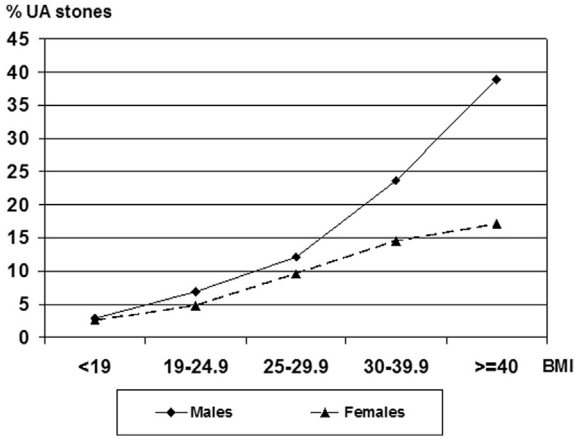

Fig. 7. Proportion of UA stones in male and female non-diabetic patients as a function of their body mass index (BMI, kg/m^2).

5. Conclusion

The complete set of PND data showed that the crystal size of UA kidney stones was significantly different between male and female patients. Moreover, type 2 diabetes altered this difference. For non-diabetic patients, the average size of UAA nanocrystals was 85 nm for male and 140 nm for female patients ($p < 10^{-5}$). For diabetic patients, the average size of UAA crystals was 76.0 nm for male subjects and 78.8 nm for female subjects ($p = 0.6$). Explanations based on differences in urine supersaturation may help to explain the observed differences, but further studies are needed to understand more precisely these structural modifications of UA kidney stones, which is in line with similar observations regarding epidemiological data.

References

[1] M. Lahti-Koski, E. Seppanen-Nuijten, S. Mannisto, T. Härkäne, H. Rissanen, P. Knekt, A. Rissanen, M. Heliövaara, Obes. Rev. 11 (2010) 171.
[2] M.C. Smith, Policy Polit. Nurs. Pract. 10 (2009) 134.
[3] J.R. Asplin, Adv. Chronic Kidney Dis. 16 (2009) 11.
[4] S.R. Bornstein, M. Ehrhart-Bornstein, M.L. Wong, J. Licinio, Exp. Clin. Endocrinol. Diabetes 116 (2008) S30.
[5] J. Cy, C. To, Int. J. Cardiol. 132 (2009) 1.
[6] A.R. Abubakari, R.S. Bhopal, Public Health 122 (2008) 173.
[7] C.F. Rueda-Clausen, F.A. Silva, P. López-Jaramillo, Int. J. Cardiol. 125 (2008) 111.
[8] G.C. Curhan, Urol. Clin. North Am. 34 (2007) 287.
[9] A. Hesse, E. Brandle, D. Wilbert, K.U. Kohrmann, P. Alken, Eur. Urol. 44 (2003) 709.
[10] A. Trinchieri, Urol. Res. 34 (2006) 151.
[11] M. Daudon, O. Traxer, E. Lechevallier, C. Saussine, Prog. Urol. 18 (2008) 802.

[12] Th Knoll, Eur. Urol. Suppl. 9 (2010) 802.
[13] Y.-T. Chen, Urological Sci. 23 (2012) 5.
[14] W.Y. Huang, Y.F. Chen, S. Carter, H.-C. Chang, C.-F. Lan, K.-H. Huang, J. Urol. 189 (2013) 2158.
[15] F.A. Kaboré, T. Kambou, B. Zango, A. Ouattara, M. Simporé, C. Lougué/Sorgho, E. Lechevalier, G. Karsenty, Prog. Urol. 23 (2013) 971.
[16] Z. El Lekhlifi, F. Laziri, H. Boumzaoued, M. Maouloua, M. Louktibi, J. Pédiatr. Puér. 27 (2014) 23.
[17] V. Castiglione, F. Jouret, O. Bruyère, B. Dubois, A. Thomas, D. Waltregny, A.-C. Bekaert, É. Cavalier, R. Gadisseur, Néphrol. Thér 11 (2015) 42.
[18] M. Lopez, B. Hoppe, Ped. Nephrol. 25 (2010) 45.
[19] M. Daudon, Ann. Urol. 39 (2005) 209.
[20] N. Meydan, S. Barutca, S. Caliskan, T. Camsari, Scand. J. Urol. Nephrol. 37 (2003) 64.
[21] E.N. Taylor, M.J. Stampfer, G.C. Curhan, Kidney Int. 68 (2005) 1230.
[22] C.M. Johnson, D.M. Wilson, W.M. O'Fallon, R.S. Malek, L.T. Kurland, Kidney Int. 16 (1979) 624.
[23] E.W. Vahlensieck, D. Bach, A. Hesse, Urol. Res. 10 (1982) 161.
[24] X. Sun, L. Shen, X. Cong, H. Zhu, J. Lv, L. He, J. Pediatr. Surgery 46 (2011) 723.
[25] Y.H. Chou, C.C. Li, W.J. Wu, Y.S. Juan, S.P. Huang, Y.C. Lee, C.C. Liu, W.M. Li, C.H. Huang, A.W. Chang, Kaohsiung J. Med. Sci. 23 (2007) 63.
[26] A.A. Shamema, K.T. Arul, R.S. Kumar, S.N. Kalkura, Spectrochim. Acta Part A 134 (2015) 442.
[27] W. Wu, D. Yang, H.-G. Tiselius, L. Ou, Y. Liang, H. Zhu, S. Li, G. Zeng, Urology 83 (2014) 732.
[28] M. Daudon, C.A. Bader, P. Jungers, Scanning Microsc. 7 (1993) 1081.
[29] Members of the French Urological Association Urolithiasis Committee P. Meria, H. Hadjadj, P. Jungers, M. Daudon, J. Urol. 183 (2010) 1412.
[30] M. Daudon, Arch. Pédiatr 7 (2000) 855.
[31] M. Daudon, O. Traxer, P. Jungers, D. Bazin, AIP Conf. Proc. 900 (2007) 26.
[32] M. Daudon, P. Jungers, D. Bazin, AIP Conf. Proc. 1049 (2008) 199.
[33] M. Daudon, P. Jungers, D. Bazin, N. Eng. J. Med. 359 (2008) 100.
[34] M. Daudon, H. Bouzidi, D. Bazin, Urol. Res. 38 (2010) 459.
[35] S. Gràcia-Garcia, F. Millán-Rodríguez, F. Rousaud-Barón, R. Montañés-Bermúdez, O. Angerri-Feu, F. Sánchez-Martín, H. Villavicencio-Mavrich, A. Oliver-Sampe, Act. Urol. Esp. 35 (2011) 354 (English Edition).
[36] E. Letavernier, O. Traxer, J.P. Haymann, D. Bazin, M. Daudon, Prog. Urol. – FMC 22 (2012) F119.
[37] M. Daudon, Prog. Urol. – FMC 22 (2012) F87.
[38] H. Bouzidi, D.P. de Brauwère, M. Daudon, Nephrol. Dial. Transpl. 26 (2011) 565.
[39] M. Livrozet, S. Vandermeersch, L. Mesnard, E. Thioulouse, J. Jaubert, J.J. Boffa, J.-Ph. Haymann, L. Baud, D. Bazin, M. Daudon, E. Letavernier, PLoS One 9 (2014) e102700.
[40] D. Bazin, J.-Ph. Haymann, E. Letavernier, J. Rode, M. Daudon, Presse Méd. 43 (2014) 135.
[41] A. Dessombz, E. Letavernier, J.-P. Haymann, D. Bazin, M. Daudon, J. Urol. 193 (2015) 1564.
[42] C.R. Powell, M.L. Stoller, B.E. Schwartz, C. Kane, D.L. Gentle, J.E. Bruce, S.W. Leslie, Urology 55 (2000) 825.
[43] C.Y. Pak, K. Sakhaee, R.D. Peterson, J.R. Poindexter, W.H. Frawley, Kidney Int. 60 (2001) 757.
[44] M. Daudon, O. Traxer, P. Conort, B. Lacour, P. Jungers, J. Am. Soc. Nephrol. 17 (2006) 2026.
[45] N.M. Maalouf, K. Sakhaee, J.H. Parks, F.L. Coe, B. Adams-Huet, C.Y. Pak, Kidney Int. 65 (2004) 1422.
[46] M. Daudon, B. Lacour, P. Jungers, Nephrol. Dial. Transpl. 20 (2005) 468.
[47] M. Daudon, P. Jungers, Feuill. Biol. 42 (2001) 37.
[48] M. Daudon, B. Lacour, P. Jungers, Urol. Res. 34 (2006) 193.
[49] C.Y. Pak, K. Sakhaee, O. Moe, G.M. Preminger, J.R. Poindexter, R.D. Peterson, P. Pietrow, W. Ekeruo, Urology 61 (2003) 523.
[50] M. Van Meerssche, J. Feneau-Dupont, Introduction à la cristallographie et à la chimie structurale, Vander, Brussels, 1973.
[51] J.D. Currey, Science 309 (2005) 253.
[52] J.Y. He, J.-M. Ouyang, R.-E. Yang, Mater. Sci. Eng. C 30 (2010) 878.
[53] D. Bazin, M. Daudon, Ch. Combes, Ch. Rey, Chem. Rev. 112 (2012) 5092.
[54] V.K. SinghPradeep, K. Rai, Biophys. Rev. 6 (2014) 291.
[55] R. Flannigan, W.H. Choy, B. Chew, D. Lange, Nat. Rev. Urol. 11 (2014) 333.
[56] J. Gómez-Morales, G. Falini, J. Manuel García-Ruiz (Eds.), Handbook of Crystal Growth, 2nd ed., 2015, pp. 873–913.
[57] V.K. Pecharsky, P.Y. Zavalij, Fundamentals of Powder Diffraction and Structural Characterization of Materials, Springer-Verlag, Berlin, 2005.
[58] D. Bazin, M. Daudon, P. Chevallier, S. Rouzière, E. Elkaim, D. Thiaudière, B. Fayard, E. Foy, P.A. Albouy, G. André, G. Matzen, E. Véron, Ann. Biol. Clin. 64 (2006) 125.
[59] D. Bazin, M. Daudon, J. Phys. D: Appl. Phys. 45 (2012) 383001.
[60] E.V. Yusenko, K.V. Yusenko, I.V. Korolkov, A.A. Shubin, F.P. Kapsargin, A.A. Efremov, M.V. Yusenko, Central Eur. J. Chem. 11 (2013) 2107.
[61] M.A. Wells, B. Hernandez-Morales, J.H. Root, E.B. Hawbolt, Phys. B Condens. Matter 241 (1997) 1274.
[62] J. Trewhella, Physica B 385–386 (2006) 825.
[63] M. Daudon, D. Bazin, G. André, P. Jungers, A. Cousson, P. Chevallier, E. Véron, G. Matzen, J. Appl. Crystallogr. 42 (2009) 109.
[64] D. Bazin, C. Chappard, C. Combes, X. Carpentier, S. Rouzière, G. André, G. Matzen, M. Allix, D. Thiaudière, S. Reguer, P. Jungers, M. Daudon, Osteoporos. Int. 20 (2009) 1065.
[65] D. Bazin, G. André, R. Weil, G. Matzen, E. Véron, X. Carpentier, M. Daudon, Urology 79 (2012) 786.
[66] D. Bazin, M. Daudon, G. André, R. Weil, E. Véron, G. Matzen, J. Appl. Crystallogr. 47 (2014) 719.
[67] F. Brisset, M. Repoux, J. Ruste, F. Grillon, F. Robaut, Scanning electron microscopy and microanalysis, EDP Sciences, 2009, ISBN 978-2-7598-0082-7.
[68] N. Quy-Dao, M. Daudon, Infrared and Raman Spectra of Calculi, Elsevier, 1997.
[69] L. Maurice-Estepa, P. Levillain, B. Lacour, M. Daudon, Clin. Chim. Acta 298 (2000) 1.
[70] http://www-llb.cea.fr/spectros/pdf/g41-llb.pdf.
[71] J. Rodríguez-Carvajal, Newsletter 26 (2001) 12.
[72] G. Artioli, N. Masciocchi, E. Galli, Acta Cryst. B 53 (1997) 498.
[73] H. Ringertz, Acta Cryst. 20 (1996) 397.
[74] J. Rodriguez-Carvajal, Physica B 192 (1993) 55.
[75] W.M. Li, Y.H. Chou, C.C. Li, C.C. Liu, S.P. Huang, W.J. Wu, C.H. Huang, Urol. Int. 82 (2009) 48.
[76] S. Ghosh, S. Basu, S. Chakraborty, A.K. Mukherjee, J. Appl. Crystallogr. 42 (2009) 629.
[77] M. Carvalho, M.A. Vieira, Intern. Braz. J. Urol. 30 (2004) 205.
[78] A. Hesse, W. Berg, C. Bothor, Intern. Urol. Nephrol. 11 (1979) 11.
[79] F. Grases, A.L. Villacampa, A. Costa Bauza, O. Sohnel, Scan. Microsc. 13 (1999) 223.
[80] P.K. Grover, R.L. Ryall, Mol. Med. 8 (2002) 525.
[81] R.J.C. Mclean, J. Downey, I. Clapham, Urol. Res. 18 (1990) 39.
[82] X. Carpentier, M. Daudon, O. Traxer, P. Jungers, A. Mazouyes, G. Matzen, E. Véron, D. Bazin, Urology 73 (2009) 968.
[83] M. Daudon, O. Traxer, J. Williams, O. Traxer, D. Bazin, in: N. Rao, J.P. Kavanagh, G.M. Preminger (Eds.), Urinary Tract Stone Disease, Springer, New York, 2011.
[84] J.C. Lieske, L.S. de la Vega, M.T. Gettman, J.M. Slezak, E.J. Bergstralh, L.J. Melton, C.L. Leibson, Am. J. Kidney Dis. 48 (2006) 897.
[85] W.O. Ekeruo, Y.H. Tan, M.D. Young, J. Urol. 172 (2004) 159.
[86] N. Abate, M. Chandalia, A.V. Cabo-Chan, O.W. Moe, Kidney Int. 65 (2004) 386.
[87] M. Daudon, Sém. Univ. Néphrol 38 (2012) 142.
[88] F.C.M. Torricelli, S. De, S. Gebreselassie, I. Li, C. Sarkissian, M. Monga, Urology 84 (2014) 544.
[89] E.S. Ford, W.H. Giles, W.H. Dietz, JAMA 287 (2002) 356.
[90] K.F. Petersen, D. Befroy, S. Dufour, Science 300 (2003) 1140.
[91] K. Sakhaee, B. Adams-Huet, O.W. Moe, C.Y. Pak, Kidney Int. 62 (2002) 971.
[92] M. Daudon, J.C. Doré, P. Jungers, B. Lacour, Urol. Res. 32 (2004) 241.
[93] R. Boistelle, Adv. Nephrol. 15 (1986) 173.
[94] W.G. Robertson, M. Peacock, P.J. Heyburn, Scand. J. Urol. 53 (1980) 199.
[95] H. Ito, T. Kotabe, K. Nomura, M. Masai, Eur. Urol. 27 (1995) 324.
[96] I.A. Bobulescu, N.M. Maalouf, G. Capolongo, B. Adams-Huet, T.R. Rosenthal, O.W. Moe, K. Sakhaee, Am. J. Physiol. Ren. Physiol. 305 (2013) F1498.
[97] M. Daudon, R. Donsimoni, C. Hennequin, S. Fellahi, G. Le Moël, M. Paris, S. Troupel, B. Lacour, Urol. Res. 23 (1995) 319.